EXPERIMENTAL INVESTIGATION OF FLOW PATTERN IN ENHANCED HEAT EXCHANGERS WITH ACTIVE INSERT DEVICES

J. P. Solano*, A. García*, J. M. Pedrero**, P. G. Vicente**, A. Viedma*,

****Departamento de Ingeniería Térmica y de Fluidos, Universidad Politécnica de Cartagena. Campus de la Muralla del Mar, 30202 Cartagena, Spain.***
Tel: +34 968 32 5938, Fax: +34 968 32 5999, e-mail address: juanp.solano@upct

*****Departamento de Ingeniería de Sistemas Industriales, Universidad Miguel Hernández.. Avenida del Ferrocarril, s/n, 03202 Elche, Spain.***

1. Summary

The present paper studies the flow features induced by a mechanically assisted device inserted in a round tube. The reciprocating movement of the active insert device generates macroscopic displacements of the flow, increasing heat transfer. At the same time, the insert device scraps the inner tube wall, avoiding fouling.

Particle Image Velocimetry technique has been employed to obtain the velocity field over a symmetry plane. In static conditions, two flow features have been identified, as well as its evolution for a range of Reynolds number between 44 and 369.

In dynamic conditions, the flow conditions for Re=44 and two different scraping velocities have been studied. The flow features for the two stages of the scraping cycle have been identified, revealing higher velocity distributions than in the static condition.

2 Introduction

Investigations on heat transfer enhancement are at present being carried out in order to obtain more efficient and low cost heat exchangers. Webb [1] classified enhancement techniques into two main groupings ,“passive” and “active”, depending on whether they need or not external power. Passive techniques have been studied by many research groups during the last thirty years and at present they are employed in commercial applications. Webb [1] assessed that active techniques can produce high heat transfer augmentations. However, there is a lack of experimental investigations on these techniques and they are seldom employed in practical applications.

Heat transfer processes in the food and chemical industries frequently deal with highly viscous liquids. The performance of heat exchangers working under these conditions is usually low, as a result of the characteristics of the encountered laminar regime. Insert devices produce a high flow mixing that increases tube-side heat transfer coefficients in laminar regime. If the insert device moves, the flow mixing will increase, yielding to a higher heat transfer.

In many heat exchangers, heat transfer surfaces may become coated with a deposit of solid material after a period of operation. This phenomenon, known as fouling, causes a reduced overall heat transfer coefficient (Bergles, [2]). Fouling increases the maintenance costs for heat exchangers and decreases their availability. Therefore, it is interesting to develop anti-fouling surfaces capable of mitigate or even eliminate this phenomena.

Mechanically assisted heat exchangers, where a heat transfer surface is periodically scraped by a moving element, might be used to increase heat transfer and avoid fouling. Equipment with rotating scraping blades are found in commercial practice: they prevent fouling and promote mixing and heat transfer. Many investigations have focused on these anti-fouling devices, studying flow pattern characteristics (Wang et al, [3]), their thermo-hydraulic performance (Goede and Jong, [4]) or scraping efficiency (Sun et al, [5]).

This work presents a visualization study carried-out on a dynamic insert device. The flow pattern is obtained by employin Particle Image Velocimetry (PIV) technique [6]. The active insert device is made up of several semi-circular elements, which are mounted on a shaft with a pitch of *5D* (Fig. 1). The whole deviced is moved alternatively along the axial direction by a hydraulic cylinder. The macroscopic displacements from the boundary layer region to the centre of the tube will be analysed and related to the heat transfer augmentation.

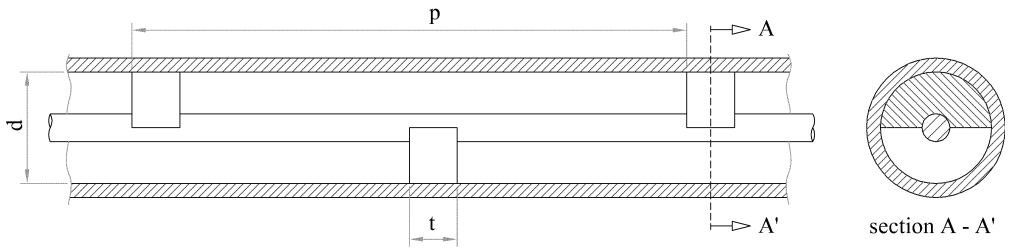

Figure 1. Sketch of the active device

3 Visualization Facility

The facility depicted in Fig. 2 was built in order to study the flow pattern induced within a device inserted inside a tube. The main section consists of a 32 mm diameter acrylic tube installed between two reservoir tanks that stabilize the flow. In the upper reservoir tank the flow temperature is regulated by an electric heater and a thermostat.

The flow is impelled from the lower calm deposit to the upper one by a gear pump, which is regulated by a frequency converter. By using mixtures of water and propylene-glycol at temperatures from 20 to 60, a Reynolds number range between 30 and 600 can be obtained.

The test section has been placed within a distance of 45 diameters from the tube inlet in order to ensure fully developed flow conditions. To improve the optical access in this section, a flat-sided acrylic box has been placed. This box was filled with the same test fluid that flows through the test section.

Particle Image Velocimetry (PIV) is a well-known technique to obtain global velocity information, instantaneously and with high accuracy. In these experiments, planar slices of the flow field that contained the axis of the pipe (longitudinal section) were illuminated, as shown in Fig. 2. The flow was seeded by 50 microns diameter polyamide particles. The camera viewed the illuminated plane from an orthogonal direction and recorded particle images at two successive instants in time in order to extract the velocity over the planar two-dimensional domain. The spatial resolution of the measurement is 0.12 mm/pixel.

A 1 mm thick light sheet is created by a pulsating diode laser of 808 nm wavelength. A computer synchronizes the camera shutter opening and the laser shot at the appropriate frequency for the test conditions. Fig. 3 shows a photograph of the set of elements.

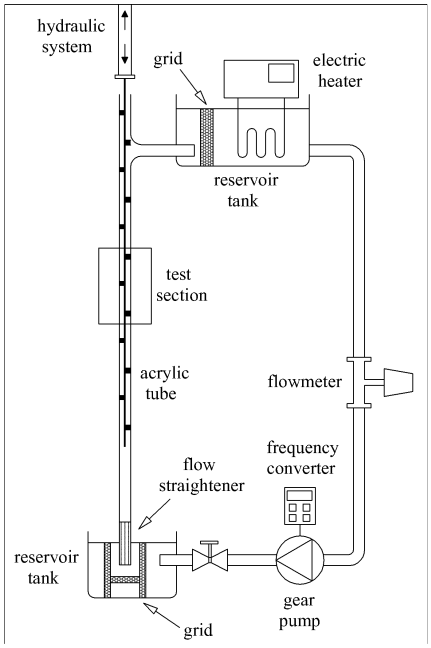

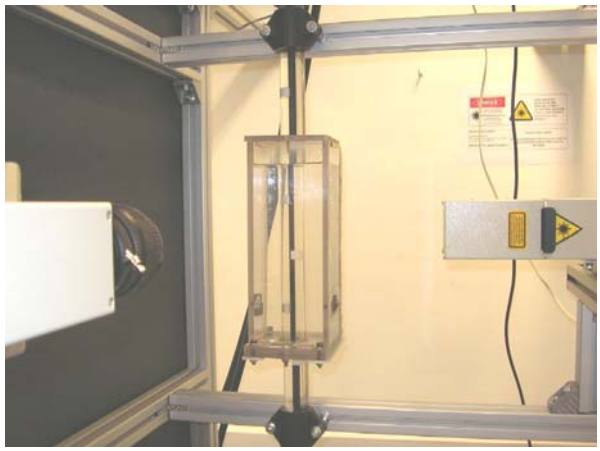

Figure 2. Sketch of the PIV facility

Figure 3. Photograph of the PIV facility

Images processing was carried out with the software vidPIV and contrasted with URAPIV, which apply a cross-correlation algorithm between consecutive images. The interrogation window size used for PIV processing was 16x16 pixels, with a 50% overlap. To obtain a clean velocity field, after the images were correlated, a global and a

local filter were applied to remove outliers. The resulting vectors were averaged over thirty realizations. Using the standard formula for 20-to-1 odds, $1.96 \cdot \sqrt{\sigma / N}$, the uncertainty in PIV measurements is about 3%. Taking into account the uncertainty in the computation of pixels displacements, the final uncertainty in PIV measurement arises to 5%.

3 Visualization Results

3.1 Static insert device

A global mean overview of the flow over one pitch of the static scraper has been carried-out. The study of the flow is conditioned by the three-dimensional geometry of the insert device inserted in a round tube. There are three main flow characteristics that help to simplify the visualization:

- There is a short entry region *(l_e=3p)*, after which the flow is considered to be periodic and fully developed.
- There is a plane of symmetry, where the main flow features can be identified. This plane has been chosen as the visualization plane: there are not velocity components normal to it. As it is shown in Fig.3, 2D PIV measurements have been performed at this plane.
- The existence of an odd plane, at both sides of which the flow structures repeat symmetrically each l_o=*p/2*.

The main flow behaviour in the symmetry plane over one pitch of the scraper is represented in Fig. 4, for different Reynolds numbers. Let us consider the mean flow in the bottom half of the tube (coming from the left of the figure). When this flow impinges the bottom plug, located at *x=p/2*, a vortex appear in the vicinity of the wall and the plug. The geometrical blockage imposed by the plug forces the flow to experience a strong deviation towards the upper half of the tube. After overcoming the obstacle, because of the sudden expansion, the flow separates, generating two symmetric recirculation bubbles in the bottom half of the tube. This recirculation bubbles merge in the symmetry plane, and they can be interpreted with PIV data from the reattachment line that separates two regions: the accelerated region, with positive *u* velocity, and the separated region, with negative *u* velocity, which provides an estimation of the recirculation bubbles dimension.

The flow in the upper half of the tube will continue accelerating towards the plug located at *x=p*, where the impingement will generate a vortex symmetric to the one described above.

In Fig 1, the dimension of the symmetric recirculation bubbles, indicated by *L*, is characterized by the distance from the first plug to the mentioned reattachment line. It can be seen that this magnitude increases with Reynolds number. It is remarkable the fact that the bubbles grow towards an asymptotic dimension, as there is little difference between this magnitude for Reynolds numbers 164 and 329.

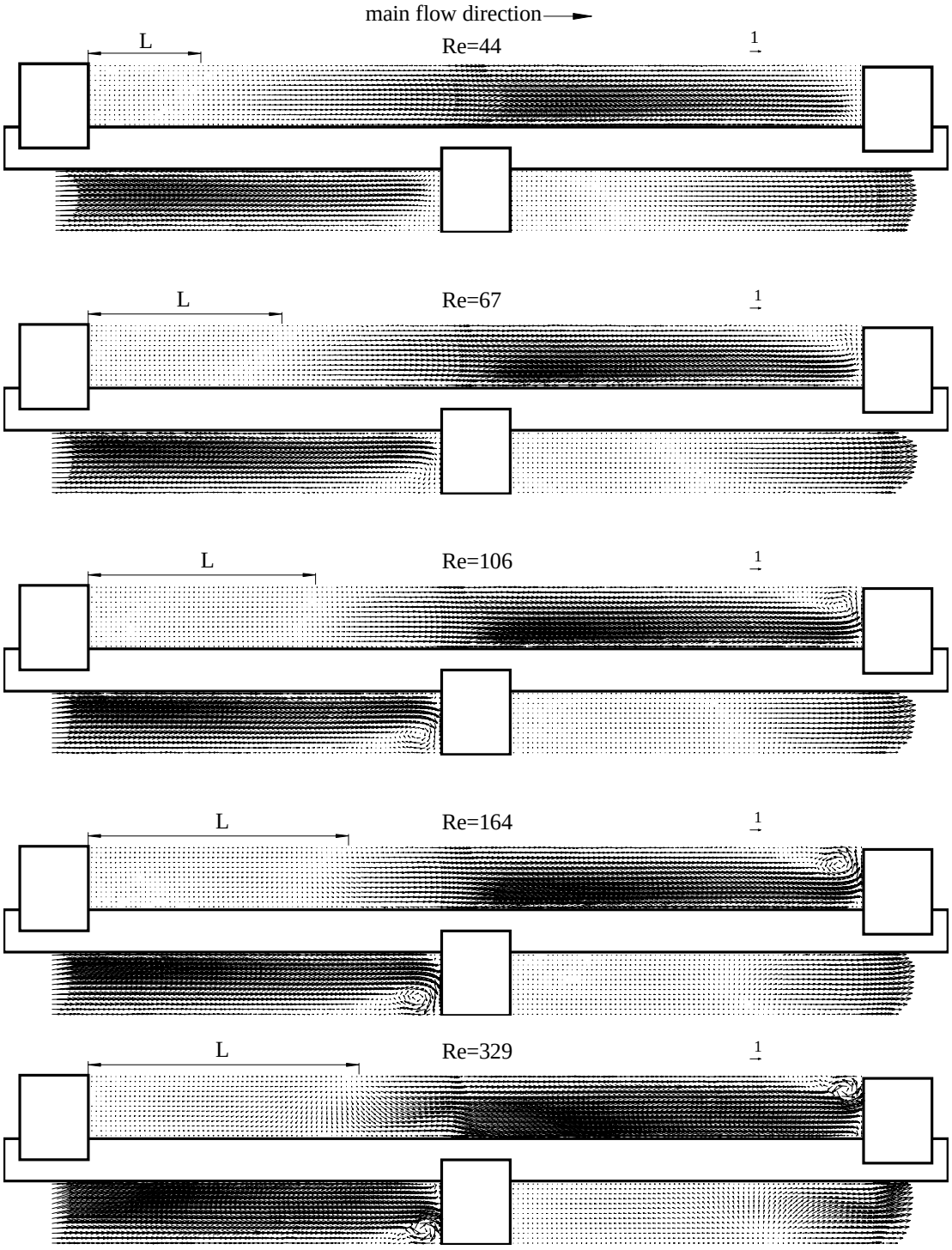

Fig.4 PIV velocity field. Static device at Reynolds numbers from 44 to 329.

The peak velocity is measured in the accelerated region. For *Re=44*, the peak velocity is 3 times the bulk velocity and at higher Reynolds numbers its value decreases (at *Re=164*, the peak velocity is 2.7 times the bulk velocity). Moreover, results show that the velocity distribution appears to be more uniform for increasing Reynolds number.

The velocity in the separated region increases for increasing Reynolds number, as shown in Fig. 4. On the other hand, a vortex grows for increasing Reynolds numbers where the accelerated flow impinges a plug. This evolution is represented in Fig. 5. At the lowest Reynolds numbers *(Re < 67)*, a region with velocity close to zero is found around the impingement area of the accelerated flow. When Reynolds number increases, a vortex appears in the plug vicinity, whose local velocities increase with Reynolds number. Moreover, a tendency to its concentration towards the tube wall is observed for *Re=329*, where a more uniform velocity profile is observed in the accelerated region.

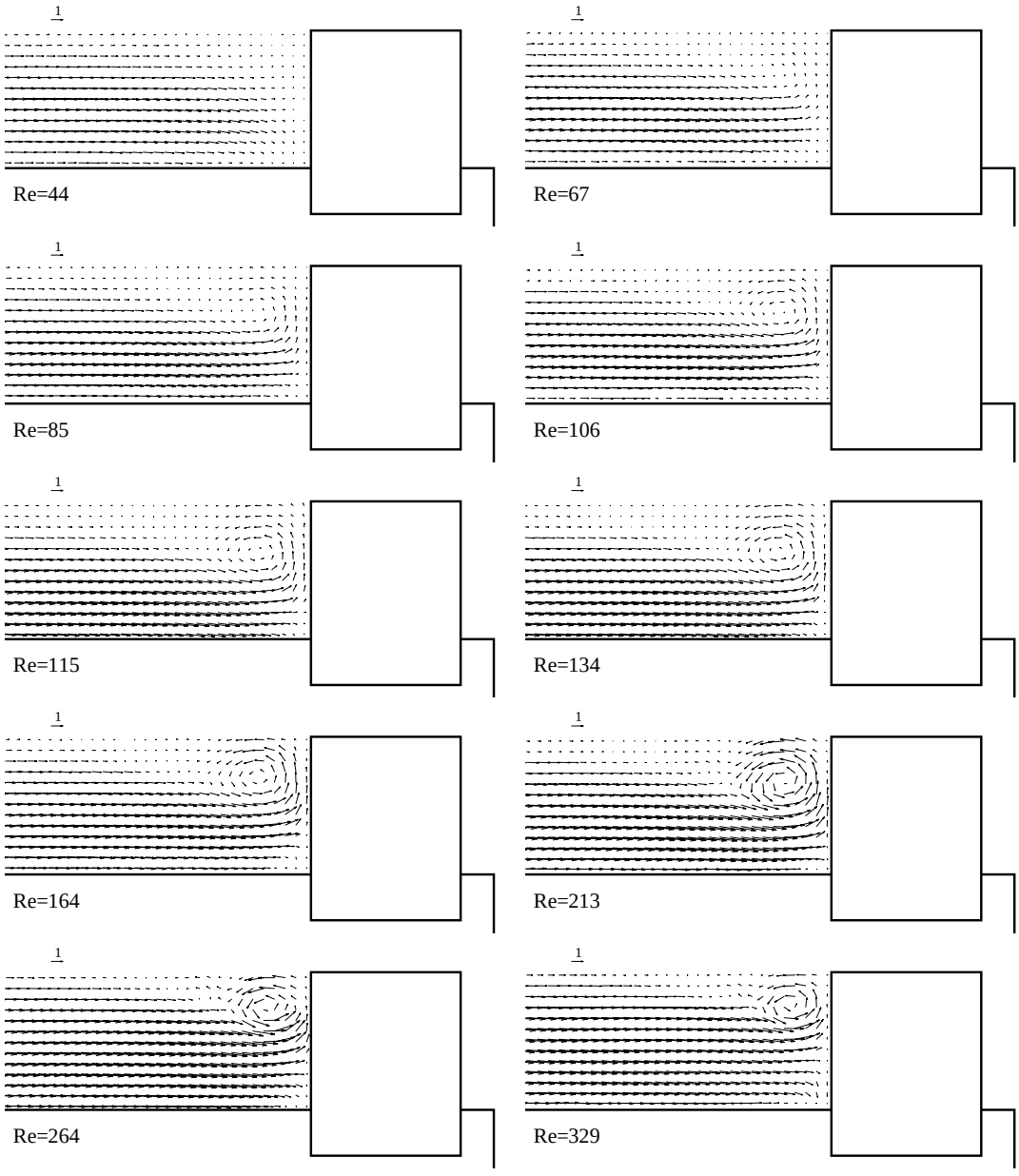

Fig.5 PIV velocity field. Static device. Flow detail upstream the semi-circular element.

3.2 Dynamic insert device

The main interest of the insert device is its reciprocating movement, which increases heat transfer and avoids fouling. This movement is achieved by means of a hydraulic unit. The pressured oil moves linearly a cylinder over which the shaft of the insert device is mounted. Two relays drive the internal open/close valve of the hydraulic unit, and the movement of the piston reverses.

In the tests carried out at the present work, the relays have been positioned in order to obtain a movement amplitude equals to the pitch of the active device ($s=p=160$ mm). Two scraping frequencies have been tested, in order to obtain scraper velocities of 3 and 4 times the bulk velocity of the fluid. For simplicity's sake, let us define the factor r as:

$$r = \frac{v_{scraper}}{v_{bulk\ fluid}}$$

The scraper velocity is constant over most of the cycle time. During each stage of the cycle, flow structures are stationary respect to the scrapper. Therefore, the flow can be considered stationary during the major part of the cycle.

To characterize this flow structures, two characteristic phases of the scraping cycle have been chosen. These two phases capture the flow structures at a position where a uniform movement of the piston is ensured; the first of them, when the piston moves in the same direction than the mean flow, and the second one when the piston moves in the direction contrary to the mean flow.

Fig. 6 shows the corresponding phase-averaged velocity fields for the two stages of the scraping cycle, for $r=3$. Fig. 7 shows similar information for $r=4$, with $Re=44$ (same fluid temperature and mass flow than in the static test at $Re=44$).

When the piston moves in the same direction than the mean flow, two regions are observed: a streamwise accelerated region, and a separated region, whose dimension is indicated by L_1. This separated region represents the existence of two symmetric recirculation bubbles. Unlike the bubbles deducted in the static measurements, these structures are higher than $p/2$. Due to the movement of the scraper in the same direction than the mean flow, no impingement of the streamwise accelerated flow exists, and thus no vortices appear in the vicinity of the plugs.

For $r=3$, peak velocities of 3.5 times the bulk velocity are found in the streamwise accelerated region, and peak velocities of 2.5 times the bulk velocity are found in the separated region.

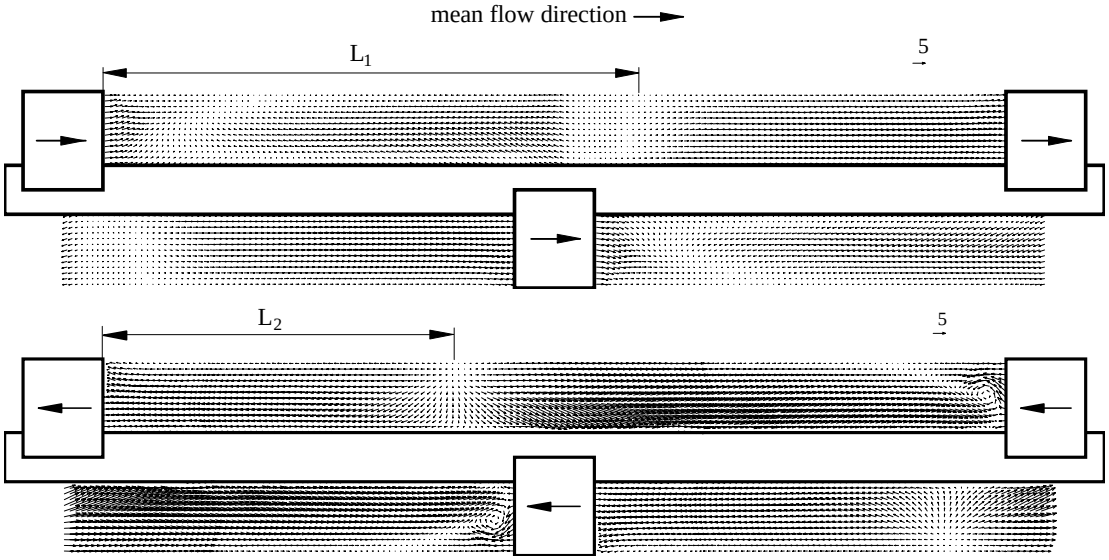

Fig. 6 PIV velocity field. Dynamic device at Reynolds numbers 44. Scraping velocity is three times the mean flow velocity (r=3).

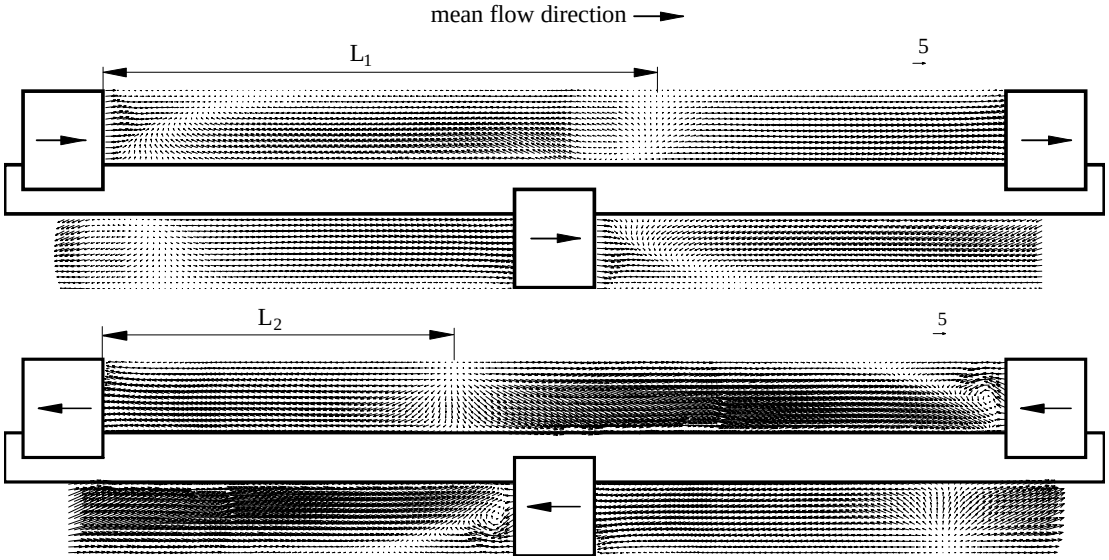

Fig. 7 PIV velocity field. Dynamic device at Reynolds numbers 44. Scraping velocity is four times the mean flow velocity (r=4).

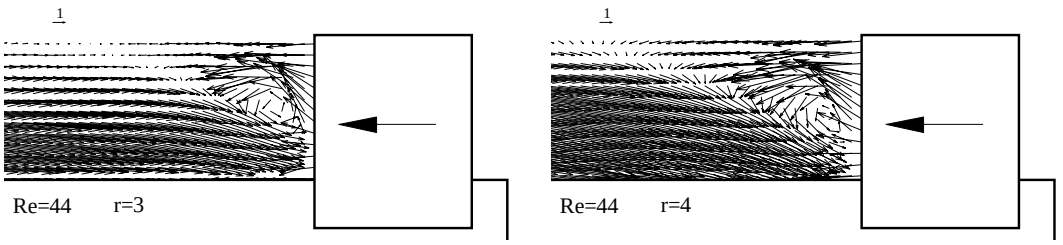

Fig. 8 PIV velocity field. Dynamic device at Reynolds numbers 44. Flow detail upstream the semi-circular element

For *r=4*, peak velocities of 5 times the bulk velocity are found in the streamwise accelerated region, and peak velocities of 3.5 times the bulk velocity are found in the separation region.

When the piston moves in the direction contrary to the mean flow, the observed flow features are similar to those found when the device is static: in this case, the impingement of the streamwise accelerated flow in a plug that moves in the contrary direction generates a vortex with high local velocities. The expansion of the flow after overcoming this plug generates two symmetric recirculation bubbles whose characteristic size is similar to the asymptotic one observed in the static measurements with high Reynolds number.

The ratio between peak velocity and fluid bulk velocity in the accelerated region is 8.5 for *r=3*, and 10.5 for *r=4*. The ratio between peak velocity and fluid bulk velocity in the separated region is also high, as a consequently of the mass flow conservation: this value is 6.5 for *r=3*, and 8.5 for *r=4*.

Fig. 8 shows the comparison of the impingement vortex for Re=44, when the insert device moves with *r=3* and with *r=4*. In comparison with the flow for the static device shown in Fig. 5, where vortex does not exist, it is clear the great influence on flow pattern produced by the insert movement.

4 Conclusions

1. Particle Image Velocimetry technique has been employed to characterize the flow features associated to an active device inserted in a round tube.

2. The static insert device has been studied, at different flow conditions that range from Reynolds numbers from 44 to 369. Two characteristic flow features have been identified, and its evolution with Reynolds number has been assessed.

3. The active insert device has been studied at Reynolds number *Re=44* and two scraping velocities. When the device moves in the same direction than the mean flow, two regions appear: a streamwise region and a separated region. When the device moves in the direction contrary to the mean flow, the observed flow features are similar to those encountered in the study of the static insert device. However, local velocities are much higher than for the static insert device.

Acknowledgements

This research has been partially financed by the DPI2003-07783-C02 grant of the "Dirección General de Investigación del Ministerio de Educación y Ciencia de España" and the “HRS Spiratube” company. We would like to thank Dr. Alexander Liberzon for his PIV program, URAPIV.

5 References

(1) R.L. Webb, “Principles of Enhanced Heat Transfer”, first ed., Wiley Interscience, New York, 1994

(2) A.E. Bergles, “ExHFT for fourth generation heat transfer technology”, Exp. Therm. Fluid Sci. 26 (2002) 335-344

(3) W. Wang, J.H. Walton, K.L. McCarthy, “Flow profiles of power law fluids in scaped surface heat exchanger geometry using MRI”, Journal of Food Process Engineering 22 (1999) 11-27

(4) R.De Goede, E.J.De Jong, “Heat transfer properties of a scraped-surface heat exhanger in the turbulent flow regime”, Chemical Engineering Science, Vol. 48, No. 8, pp.1393-1404, (1993)

(5) K.-H. Sun, D.L. Pyle, A.D. Fitt, C.P. Please, M.J. Baines, N. Hall-Taylor, “Numerical study of 2D heat transfer in a scraped surface heat exchanger”, Computers & Fluids 33 (2004) 869-880

(6) M. Raffel, C. Willert, J. Kompenahns, “Particle Image Velocimetry. A Practical Guide”. Published by Springer, Berlin, Heidelberg, 1998